

Exact Numerical Calculation of the Density of States of the Fluctuating Gap Model

Lorenz Bartosch and Peter Kopietz

Institut für Theoretische Physik, Universität Göttingen, Bunsenstrasse 9, D-37073 Göttingen, Germany
(August 4, 1999)

We develop a powerful numerical algorithm for calculating the density of states $\rho(\omega)$ of the fluctuating gap model, which describes the low-energy physics of disordered Peierls and spin-Peierls chains. We obtain $\rho(\omega)$ with unprecedented accuracy from the solution of a simple *initial value problem* for a single Riccati equation. Generating Gaussian disorder with large correlation length ξ by means of a simple Markov process, we present a quantitative study of the behavior of $\rho(\omega)$ in the pseudogap regime. In particular, we show that in the commensurate case and in the absence of forward scattering the pseudogap is overshadowed by a Dyson singularity below a certain energy scale ω^* , which we explicitly calculate as a function of ξ .

PACS numbers: 71.23.-k, 02.50.Ey, 71.10.Pm

The fluctuating gap model (FGM) describes the low-energy physics of one-dimensional fermions subject to static disorder potentials. The first quantized Hamiltonian of the FGM can be written as [1]

$$\hat{H} = -iv_F \partial_x \sigma_3 + V(x) \sigma_0 + \Delta(x) \sigma_+ + \Delta^*(x) \sigma_- , \quad (1)$$

where $V(x)$ and $\Delta(x)$ are random potentials describing forward and backward scattering, v_F is the Fermi velocity (henceforth we set $v_F = 1$), σ_i are the usual Pauli matrices, σ_0 is the 2×2 unit matrix, and $\sigma_{\pm} = \frac{1}{2}(\sigma_1 \pm i\sigma_2)$. Eq.(1) emerges as the effective low-energy Hamiltonian in different physical contexts. For example, fluctuation effects close to the Peierls transition in quasi-one-dimensional charge-density wave systems can be described by this Hamiltonian. In this case $\Delta(x)$ describes the time-independent part of the fluctuating Peierls order parameter, the probability distribution of which can be obtained from a Ginzburg-Landau expansion of the free energy [2]. For commensurate chains $\Delta(x)$ can be chosen to be real, whereas it is complex in the incommensurate case [1–3]. Truncating the Ginzburg-Landau expansion at the second order, $\Delta(x)$ is approximated by a Gaussian random process, with finite average $\langle \Delta(x) \rangle = \Delta_{av}$ below the Peierls transition and $\Delta_{av} = 0$ in the disordered phase. For commensurate chains the correlator of $\hat{\Delta}(x) = \Delta(x) - \Delta_{av}$ is $\langle \hat{\Delta}(x) \hat{\Delta}(x') \rangle = \Delta_s^2 e^{-|x-x'|/\xi}$, whereas in the incommensurate case $\langle \hat{\Delta}(x) \hat{\Delta}^*(x') \rangle = \Delta_s^2 e^{-|x-x'|/\xi}$ and $\langle \hat{\Delta}(x) \hat{\Delta}(x') \rangle = 0$. Here ξ is the order parameter correlation length, which diverges at the Peierls transition. The Hamiltonian (1) describes also the low-energy physics of disordered spin chains [1,4], which can be mapped onto disordered fermions by means of the usual Jordan-Wigner transformation. In many cases the

filling of the effective fermionic system is then commensurate with the lattice, so that $\Delta(x)$ is real.

The fundamental quantity which determines the thermodynamics of the model (1) is the density of states (DOS) $\rho(\omega)$. In general, one has to rely on approximations to calculate $\rho(\omega)$ or its disorder average $\langle \rho(\omega) \rangle$, but in special limits exact results are available. Besides the trivial case where $V(x)$ and $\Delta(x)$ are constant, the exact $\langle \rho(\omega) \rangle$ can be obtained by various methods [5–7] in the white noise limit $\xi \rightarrow 0$, $\Delta_s \rightarrow \infty$, with $\Delta_s^2 \xi \rightarrow \text{const.}$ For real $\Delta(x)$ and $V(x) = 0$ the average DOS is known to exhibit, for sufficiently small Δ_{av} , a Dyson singularity [8] at $\omega = 0$. In Ref. [9] we have shown that this singularity survives for arbitrary $\xi < \infty$. A recursive algorithm due to Sadovskii [10] does not reproduce the Dyson singularity, so that this algorithm cannot be exact. In fact, a subtle flaw in this algorithm has recently been found by Tchernyshyov [3]. Because Sadovskii's algorithm (or generalizations of it) has been used in different contexts, e.g. to explain the pseudogap phenomenon in the normal state of the cuprate superconductors [11,12], it is also important to investigate its validity for complex $\Delta(x)$ with quasi-long-range correlations.

In this work we develop an accurate algorithm which allows us to investigate the regime $\Delta_s \xi \gtrsim 1$ where no exact solution is available. We find that in the commensurate case the pseudogap is overshadowed by a Dyson singularity below a cross-over energy ω^* , which we determine as a function of the correlation length ξ . We also consider the incommensurate case for which Sadovskii's solution turns out to be qualitatively correct but leads to a wrong ξ -dependence of the depth of the pseudogap.

Riccati equation.— In the following we use the special symmetries of the continuum model (1) to show that the DOS can be obtained *without ever calculating the eigenvalues of \hat{H}* [13]. Instead, we obtain the DOS from the solution of a simple *initial value problem* for a Riccati equation. This will enable us to calculate $\rho(\omega)$ with unprecedented numerical accuracy. For a given realization of the disorder the local DOS of the Hamiltonian (1) can be defined by [9,14]

$$\rho(x, \omega) = -\pi^{-1} \text{ImTr}[\sigma_3 \mathcal{G}^R(x, x, \omega)] , \quad (2)$$

where the retarded 2×2 matrix Green function $\mathcal{G}^R(x, x', \omega)$ satisfies

$$[i\partial_x - M(x, \omega + i0^+)] \mathcal{G}^R(x, x', \omega) = \delta(x - x') \sigma_0 , \quad (3)$$

$$M(x, \omega) = [V(x) - \omega + \Delta(x) \sigma_+ + \Delta^*(x) \sigma_-] \sigma_3 . \quad (4)$$

We now make the non-Abelian Schwinger-ansatz [9,15]

$$\mathcal{G}^R(x, x', \omega) = U(x, \omega) \mathcal{G}_0^R(x - x') U^{-1}(x', \omega), \quad (5)$$

where $U(x, \omega)$ is an invertible 2×2 matrix and $\mathcal{G}_0^R(x)$ is the Green function to the operator $i\partial_x + i0^+\sigma_3$, i.e.

$$\mathcal{G}_0^R(x) = -i \begin{pmatrix} \theta(x) & 0 \\ 0 & -\theta(-x) \end{pmatrix}. \quad (6)$$

In the following the ω -dependence is suppressed. The ansatz (5) indeed solves Eq.(3) if $U(x)$ satisfies

$$[i\partial_x - M(x)] U(x) = 0 \quad (7)$$

with the boundary conditions

$$U_{12}(-\infty) = U_{21}(\infty) = 0. \quad (8)$$

Two different solutions of Eq.(7) are given by

$$U_+(x) = \text{Texp}[-i \int_{-\infty}^x M(y) dy], \quad (9)$$

$$U_-(x) = T^{-1} \text{exp}[i \int_x^{\infty} M(y) dy], \quad (10)$$

where Texp is the path-ordered and $T^{-1}\text{exp}$ is the anti-path-ordered exponential function. Because $M^\dagger = \sigma_3 M \sigma_3$ and $\text{Tr} M = 0$, the matrices U_α satisfy $U_\alpha^\dagger = \sigma_3 U_\alpha^{-1} \sigma_3$ and $\det U_\alpha = 1$, which means that they belong to the non-compact group $SU(1, 1)$. Thus, the elements of the U_α satisfy $U_{\alpha 22} = U_{\alpha 11}^*$, $U_{\alpha 12} = U_{\alpha 21}^*$, and $|U_{\alpha 11}|^2 - |U_{\alpha 21}|^2 = 1$. While each $U_\alpha(x)$ only obeys one of the two conditions (8), the combination

$$U(x) \equiv \frac{1}{\sqrt{u}} \begin{pmatrix} U_{-11}(x) & U_{+12}(x) \\ U_{-21}(x) & U_{+22}(x) \end{pmatrix}, \quad (11)$$

satisfies both boundary conditions. Here $u = U_{-11}(-\infty) = U_{+22}(\infty)$, so that $\det U(x) = 1$. Denoting the first column of the matrix U_α by \mathbf{u}_α and the second column by \mathbf{v}_α (so that $\mathbf{v}_\alpha = \sigma_1 \mathbf{u}_\alpha^*$), we obtain from Eqs.(5) and (11)

$$\mathcal{G}^R(x, x', \omega) = -i \left\{ \theta(x - x') \frac{\mathbf{u}_-(x) \mathbf{u}_+^\dagger(x')}{u} + \theta(x' - x) \frac{\mathbf{v}_+(x) \mathbf{v}_-^\dagger(x')}{u} \right\} \sigma_3. \quad (12)$$

Here \mathbf{u}_+^\dagger constitutes adjungation of \mathbf{u}_+ , so that $\mathbf{u}_- \mathbf{u}_+^\dagger$ is a 2×2 -matrix. Equivalent but more complicated forms of Eq.(12) were first derived by Abrikosov and Ryzhkin [16]. Combining Eqs.(2) and (12), we get

$$\rho(x, \omega) = \frac{1}{\pi} \text{Re} \frac{U_{-11} U_{+11}^* + U_{-21} U_{+21}^*}{U_{-11} U_{+11}^* - U_{-21} U_{+21}^*}. \quad (13)$$

Since this expression only depends on the ratios $\Phi_\alpha(x) \equiv -i U_{\alpha 21}^*(x) / U_{\alpha 11}(x)$, we may also write

$$\rho(x, \omega) = \frac{1}{\pi} \text{Re} \frac{1 + \Phi_+(x) \Phi_-^*(x)}{1 - \Phi_+(x) \Phi_-^*(x)}. \quad (14)$$

Using Eq.(7) we find that the $\Phi_\alpha(x)$ are both solutions of the same Riccati equation,

$$\partial_x \Phi_\alpha(x) = 2i\tilde{\omega}(x) \Phi_\alpha(x) + \Delta(x) - \Delta^*(x) \Phi_\alpha^2(x), \quad (15)$$

where we have introduced $\tilde{\omega}(x) = \omega - V(x)$. Similar Riccati equations have recently been obtained by Schopohl [17] from the Eilenberger equations of superconductivity. To specify the initial conditions, let us assume that outside the interval $[0, L]$ the potentials $V(x)$ and $\Delta(x)$ are real constants, V_∞ and Δ_∞ . From the definition of Φ_α we find that Eq.(15) should then be integrated with the initial conditions

$$\Phi_+(0) = \Phi_-(L) = \sqrt{1 - \frac{(\omega - V_\infty)^2}{\Delta_\infty^2}} + i \frac{\omega - V_\infty}{\Delta_\infty}, \quad (16)$$

where the square root has to be taken such that for $\Delta_\infty \rightarrow 0$ the right-hand side of Eq.(16) vanishes. Note that the initial values are simply given by the stable stationary solution of the Riccati equation (15) with $V(x) = V_\infty$ and $\Delta(x) = \Delta_\infty$.

The case of a discrete spectrum.— For $(\omega - V_\infty)^2 < \Delta_\infty^2$ the spectrum turns out to be discrete [18]: Introducing $\varphi_\alpha(x)$ via $\Phi_\alpha(x) \equiv e^{i\varphi_\alpha(x)}$ the phases satisfy

$$\partial_x \varphi_\alpha(x) = 2\tilde{\omega}(x) - 2|\Delta(x)| \sin(\varphi_\alpha(x) - \vartheta(x)), \quad (17)$$

where we have written $\Delta(x) = |\Delta(x)| e^{i\vartheta(x)}$. Because $|\Phi_+(0)| = |\Phi_-(L)| = 1$ for $(\omega - V_\infty)^2 < \Delta_\infty^2$, the initial values $\varphi_+(0)$ and $\varphi_-(L)$ are real. Hence the solutions of Eq.(17) remain real, which implies that $|\Phi_\alpha(x)| = 1$ for all x . From Eq.(16) we obtain for the initial values

$$\tan \varphi_+(0) = \tan \varphi_-(L) = \frac{\omega - V_\infty}{\sqrt{\Delta_\infty^2 - (\omega - V_\infty)^2}}. \quad (18)$$

Note that the $\varphi_\alpha(x)$ are unreduced phases which are not limited to take values between 0 and 2π . In terms of the $\varphi_\alpha(x)$ the local DOS can be written as

$$\begin{aligned} \rho(x, \omega) &= -\frac{1}{\pi} \text{Im} \cot \left(\frac{\varphi_+(x) - \varphi_-(x)}{2} + i0 \right) \\ &= 2 \sum_{m=-\infty}^{\infty} \delta(\varphi_+(x) - \varphi_-(x) - 2\pi m). \end{aligned} \quad (19)$$

We now make the ω -dependence of $\varphi_\alpha(x)$ explicit again. Since the right hand side of Eq.(17) is a 2π -periodic function of $\varphi_\alpha(x)$ it follows that if $\varphi_+(x, \omega) - \varphi_-(x, \omega) = 2\pi m$ for one x , this must also be true for all x . This implies that only for discrete values of ω does Eq.(19) yield a contribution to the local DOS. We get a delta-peak contribution to the total DOS if $\varphi_+(L, \omega) = 2\pi m + \varphi_+(0, \omega)$, where $\varphi_+(0, \omega) = \varphi_-(L, \omega)$ is given by Eq.(18). Since $\partial_\omega \varphi_+(x, \omega) > 0$, the integrated total DOS is given by

$$\mathcal{N}(\omega) = \frac{1}{L} \left[\frac{\varphi_+(L, \omega) - \varphi_+(L, 0)}{2\pi} - C(\omega) \right]_{\text{int}}, \quad (20)$$

where $[z]_{\text{int}}$ gives the integer value of z , and $C(\omega) = (\varphi_+(0, \omega) - \varphi_+(0, 0))/2\pi$ is a finite size correction of order unity that depends on the initial condition. For *real* $\Delta(x)$, a similar equation has been derived by Lifshits, Gredeskul, and Pastur [6] within the phase formalism. While these authors use a rather unphysical boundary condition, we can cope with arbitrary Δ_∞ and V_∞ . In the thermodynamic limit the integrated DOS is independently of the boundary conditions given by

$$\mathcal{N}(\omega) = \lim_{L \rightarrow \infty} (\varphi_+(L, \omega) - \varphi_+(L, 0))/2\pi L. \quad (21)$$

For large frequencies we recover the classical high-frequency limit $\mathcal{N}_0(\omega) = \omega/\pi$, so that the DOS $\rho(\omega) = \partial_\omega \mathcal{N}(\omega)$ is given by $\rho_0 = 1/\pi$. The white noise limit is also easily recovered: in this case Eq.(17) implies that the probability distribution of $\varphi_+(x)$ satisfies a Fokker-Planck equation, which was first solved by Ovchinnikov and Erikhman [5] for the commensurate case. For the most general case with complex $\Delta(x)$ see Ref. [7].

Numerical algorithm.— In the following we present an exact algorithm which allows to numerically calculate the (integrated) DOS for stepwise constant potentials. By choosing the step size sufficiently small, arbitrarily given potentials may be approximated in this way. Assuming that in the open intervals $[x_n, x_{n+1}[$ the potentials $\Delta(x)$ and $V(x)$ are given by the constants Δ_n and V_n , the matrix $U_+(x)$ can be written as a finite product of matrices of the form

$$e^{-iM_n \delta_n} \equiv \begin{pmatrix} t_n & i r_n^* \\ -i r_n & t_n^* \end{pmatrix} = \cosh[\sqrt{|\Delta_n|^2 - \tilde{\omega}_n^2} \delta_n] \sigma_0 + i \sinh[\sqrt{|\Delta_n|^2 - \tilde{\omega}_n^2} \delta_n] \frac{\Delta_n \sigma_+ - \Delta_n^* \sigma_- + \tilde{\omega}_n \sigma_3}{\sqrt{|\Delta_n|^2 - \tilde{\omega}_n^2}}, \quad (22)$$

where $\tilde{\omega}_n = \omega - V_n$ and $\delta_n = x_{n+1} - x_n$. For the Riccati variable $\Phi_+(x)$ satisfying Eq.(15) this implies the recurrence relation

$$\Phi_+(x_{n+1}) = \frac{r_n^* + t_n \Phi_+(x_n)}{t_n^* + r_n \Phi_+(x_n)}. \quad (23)$$

We found that for a given realization of Δ_n and V_n it is easier to calculate the dynamics of $\Phi_+(x)$ and to keep track of its phase than to directly solve Eq.(17). Whenever $\text{Re}\Phi_+(x) > 0$ and there is a sign change in $\text{Im}\Phi_+(x)$, the winding number $[\varphi_+(x)/2\pi]_{\text{int}}$ is changed by one. To detect all such changes we demand that the length δ_n of all intervals satisfies $2(|\tilde{\omega}_n| + |\Delta_n|)\delta_n < \pi/2$. Since very long chains show a self-averaging effect, we only need to simulate one typical chain to obtain the average DOS.

To generate Gaussian disorder with correlation length ξ we have found the following realization of an Ornstein-Uhlenbeck process [19], which is much simpler than the algorithm proposed in Ref. [3]. Using the Box-Muller algorithm [20], we generate independent Gaussian random numbers g_n with $\langle g_n \rangle = 0$ and $\langle g_n^2 \rangle = 1$. For real $\Delta(x)$ we set $\Delta_n = \Delta_{\text{av}} + \tilde{\Delta}_n$ and generate the $\tilde{\Delta}_n$ recursively according to

$$\tilde{\Delta}_0 = \Delta_s g_0, \quad \tilde{\Delta}_{n+1} = a_n \tilde{\Delta}_n + \sqrt{1 - a_n^2} \Delta_s g_{n+1}, \quad (24)$$

where $a_n = e^{-|\delta_n|/\xi}$. It is straightforward to show that this Markov process indeed leads to a Gaussian random process with the desired properties. Obvious advantages of our algorithm are that the random variables Δ_n can be generated simultaneously with the iteration of the recurrence relation (23), and that Δ_{n+1} depends only on the previous Δ_n , so that the implementation of this algorithm requires practically no memory space. Of course, our algorithm can also be used to generate V_n , and in the complex case $\text{Re}\Delta_n$ and $\text{Im}\Delta_n$ can be generated by replacing Δ_s by $\Delta_s/\sqrt{2}$.

Results.— In Fig.1 we show our numerical results for $\rho(\omega)/\rho_0$ for $V(x) = \Delta_{\text{av}} = 0$ and real $\Delta(x)$. Except for $\Delta_s \xi = 1000, 0.2$ we have chosen the same values of the dimensionless parameter $\Delta_s \xi$ as in Fig.7 of Ref. [10]. One clearly sees the Dyson singularity, which exists for any finite value of ξ and overshadows the pseudogap at sufficiently small energies. This Dyson singularity is missed by Sadovskii's algorithm [10]. On the other hand, for complex $\Delta(x)$ this algorithm turns out to be qualitatively correct which can be seen by comparing our data in Fig.2 with those in Fig.5 of Ref. [10]. For a more quantitative comparison, the triangles (real $\Delta(x)$) and diamonds (complex $\Delta(x)$) in Fig.3 show the DOS $\rho(\omega^*)$ at the energy ω^* where $\rho(\omega)$ assumes its minimum. Note that in the incommensurate case $\omega^* = 0$. The numerical errors (which are mainly due to the finite length of the chain) are smaller than the size of the symbols. The straight lines are fits to power-laws $\rho(\omega^*)/\rho_0 = A(\Delta_s \xi)^{-\mu}$. For real $\Delta(x)$ we obtain $A = 0.482 \pm 0.010$, $\mu = 0.3526 \pm 0.0043$, while for complex $\Delta(x)$ our result is $A = 0.6397 \pm 0.0066$ and $\mu = 0.6397 \pm 0.0024$, i.e. within numerical accuracy we find $A = \mu$. The circles in Fig.3 show for real $\Delta(x)$ the energy scale ω^* where $\rho(\omega)$ is minimal. The long solid line is a fit to a power-law $\omega^*/\Delta_s = B(\Delta_s \xi)^{-\gamma}$, with $B = 0.2931 \pm 0.0074$ and $\gamma = 0.3513 \pm 0.0051$. Here we find within numerical accuracy $\mu = \gamma$. The proportionality of $\rho(\omega^*)$ to the energy scale ω^* , which can be interpreted as the width of the Dyson singularity, can also directly be seen in Fig.1. Finally we note that for $\Delta_s \xi \lesssim 0.2$ our algorithm produces results consistent with the white noise limit $\Delta_s \xi \ll 1$. While $\rho(0) \rightarrow 1$ in the incommensurate case, in the commensurate case we obtain from the exact solution of Ovchinnikov and Erikhman [5] $\rho(\omega^*)/\rho_0 \rightarrow 0.9636$, and $\omega^* \rightarrow 1.2514 \Delta_s^2 \xi$, which determines the short solid line in Fig.3 describing $\omega^*(\xi)$ in the white-noise limit.

Summary.— We have developed a powerful numerical algorithm to calculate the average DOS of the FGM with very high accuracy. The algorithm can be used for arbitrary forward and backward scattering potentials, so that it is not restricted to the case of vanishing averages and Gaussian statistics which we further considered in this work. Our main results are: (a) for commensurate chains in the absence of forward scattering the DOS exhibits for

large ξ a pseudogap and a Dyson singularity. We have explicitly calculated the width of the Dyson singularity as a function of ξ . The most promising experimental systems to detect Dyson singularities are spin chains [1]. (b) In the incommensurate case the algorithm proposed by Sadovskii [10] is qualitatively correct. However, his result $\langle \rho(0) \rangle \propto \xi^{-1/2}$ is incorrect. This should be kept in mind for a quantitative comparison between experimental data [11] and calculations based on Sadovskii's algorithm.

We thank K. Schönhammer for discussions. This work was financially supported by the DFG (Grants No. Ko 1442/3-1 and Ko 1442/4-1).

-
- [1] J. E. Bunder and R. H. McKenzie, Phys. Rev. B **60**, 344 (1999).
 - [2] P. A. Lee, T. M. Rice, and P. W. Anderson, Phys. Rev. Lett. **31**, 462 (1973).
 - [3] O. Tchernyshyov, Phys. Rev. B **59**, 1358 (1999).
 - [4] R. H. McKenzie, Phys. Rev. Lett. **77**, 4804 (1996); M. Fabrizio and R. Mélin, Phys. Rev. Lett. **78**, 3382 (1997); M. Steiner *et al.*, Phys. Rev. B **57**, 8290 (1998);
 - [5] A. A. Ovchinnikov and N. S. Erikhman, Zh. Eksp. Teor. Fiz. **73**, 650 (1977) [Sov. Phys. JETP **46**, 340 (1977)].
 - [6] I. M. Lifshits, S. A. Gredeskul, and L. A. Pastur, *Introduction to the Theory of Disordered Systems*, (Wiley, New York, 1988).
 - [7] R. Hayn and J. Mertsching, Phys. Rev. B **54**, R5199 (1996).
 - [8] F. J. Dyson, Phys. Rev. **92**, 1331 (1953).
 - [9] L. Bartosch and P. Kopietz, Phys. Rev. Lett. **82**, 988 (1999).
 - [10] M. V. Sadovskii, Zh. Eksp. Teor. Fiz. **77**, 2070 (1979) [Sov. Phys. JETP **50**, 989 (1979)].
 - [11] J. Schmalian *et al.*, Phys. Rev. Lett. **80**, 3839 (1998); Phys. Rev. B **60**, 667 (1999).
 - [12] R. H. McKenzie and D. Scarratt, Phys. Rev. B **54**, R12709 (1996).
 - [13] While this work was prepared for publication, a preprint appeared (A. Millis and H. Monien, cond-mat/9907233), in which the DOS of the FGM was calculated numerically from exact diagonalizations of lattice regularizations of Eq.(1). Our results partially disagree with those of Millis and Monien.
 - [14] We measure energies relative to the Fermi energy and set the Fermi velocity and \hbar equal to unity.
 - [15] J. Schwinger, Phys. Rev. **128**, 2425 (1962). Note that in contrast to Ref. [9] $\mathcal{G}_0^R(x)$ is independent of ω and therefore the matrix $U(x, \omega)$ is also different.
 - [16] A. A. Abrikosov and I. A. Ryzhkin, Zh. Eksp. Teor. Fiz. **71**, 1204 (1976) [Sov. Phys. JETP **44**, 630 (1976)].
 - [17] N. Schopohl, cond-mat/9804064.
 - [18] In Ref. [9] we have calculated the exact $\rho(x, \omega = 0^+)$ for $V(x) = \Delta_\infty = 0$ and real $\Delta(x)$. In this case $\Phi_+(0) = \Phi_-(L) = 0$, and the spectrum is continuous.
 - [19] L. Bartosch, (unpublished).
 - [20] W. H. Press *et al.*, *Numerical Recipes in C*, (2nd ed., Cambridge University Press, Cambridge, 1992).

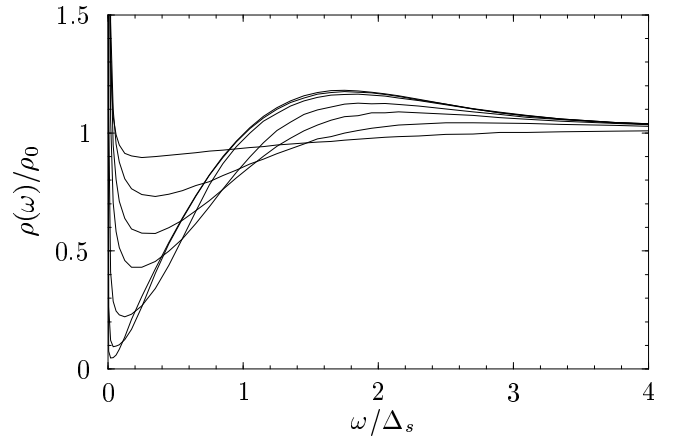


FIG. 1. Average DOS for real $\Delta(x)$ with $\Delta_s L = 10^7$, $V(x) = \Delta_{av} = 0$, and $\Delta_s \xi = 1000, 100, 10, 2, 1, 0.5, 0.2$. The minimal DOS $\rho(\omega^*)$ decreases with increasing $\Delta_s \xi$.

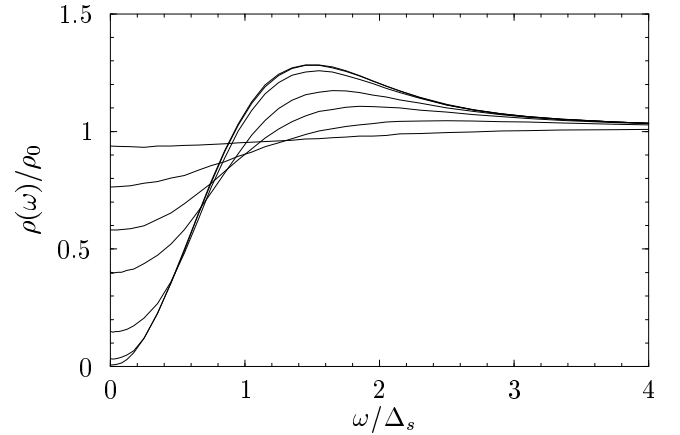


FIG. 2. Average DOS for complex $\Delta(x)$ with $\Delta_s L = 10^7$, $V(x) = \Delta_{av} = 0$, and $\Delta_s \xi = 1000, 100, 10, 2, 1, 0.5, 0.2$. $\rho(0)$ decreases with increasing $\Delta_s \xi$.

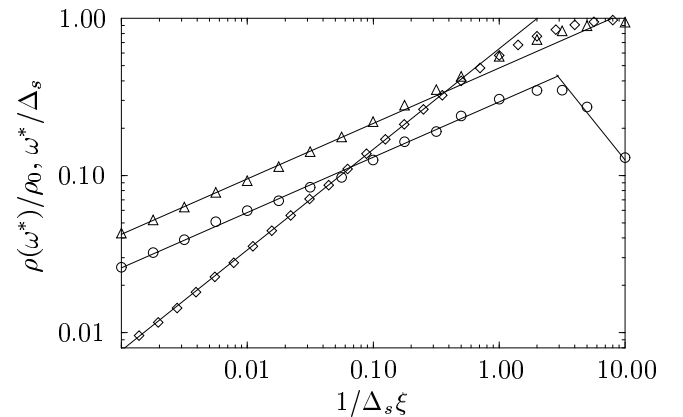


FIG. 3. Double-logarithmic plot of $\rho(\omega^*)/\rho_0$ as a function of $1/\Delta_s \xi$ for real $\Delta(x)$ (triangles) and complex $\Delta(x)$ (diamonds), where ω^* is the energy for which the DOS assumes its minimum. While $\omega^* = 0$ for complex $\Delta(x)$, the circles give the double-logarithmic plot of ω^*/Δ_s for real $\Delta(x)$ as a function of $1/\Delta_s \xi$.